

# Transcranial Optical Monitoring of Cerebral Hemodynamics in Acute Stroke Patients during Mechanical Thrombectomy

Rodrigo M. Forti, MSc,<sup>\*†‡,††</sup> Christopher G. Favilla, MD,<sup>§,††</sup>  
 Jeffrey M. Cochran, PhD,<sup>‡</sup> Wesley B. Baker, PhD,<sup>||</sup> John A. Detre, MD,<sup>§,\*\*</sup>  
 Scott E. Kasner, MD,<sup>§</sup> Michael T. Mullen, MD,<sup>§</sup> Steven R. Messé, MD,<sup>§</sup>  
 W. Andrew Kofke, MD,<sup>¶</sup> Ramani Balu, MD, PhD,<sup>§</sup> David Kung, MD,<sup>#,\*\*</sup>  
 Bryan A. Pukenas, MD,<sup>#,\*\*</sup> Neda I. Sedora-Roman, MD,<sup>\*\*</sup>  
 Robert W. Hurst, MD,<sup>#,\*\*</sup> Omar A. Choudhri, MD,<sup>#</sup>  
 Rickson C. Mesquita, PhD,<sup>\*†</sup> and Arjun G. Yodh, PhD<sup>‡</sup>

*Introduction:* Mechanical thrombectomy is revolutionizing treatment of acute stroke due to large vessel occlusion (LVO). Unfortunately, use of the modified Thrombolysis in Cerebral Infarction score (mTICI) to characterize recanalization of the cerebral vasculature does not address microvascular perfusion of the distal parenchyma, nor provide more than a vascular “snapshot.” Thus, little is known about tissue-level hemodynamic consequences of LVO recanalization. Diffuse correlation spectroscopy (DCS) and diffuse optical spectroscopy (DOS) are promising methods for continuous, noninvasive, contrast-free transcranial monitoring of cerebral microvasculature. *Methods:* Here, we use a combined DCS/DOS system to monitor frontal lobe hemodynamic changes during endovascular treatment of 2 patients with ischemic stroke due to internal carotid artery (ICA) occlusions. *Results and Discussion:* The monitoring instrument identified a recanalization-induced increase in ipsilateral cerebral blood flow (CBF) with little or no concurrent change in contralateral CBF and extracerebral blood flow. The results suggest that diffuse optical monitoring is sensitive to intracerebral hemodynamics in patients with ICA occlusion and can measure microvascular responses to mechanical thrombectomy.

**Key Words:** Cerebral blood flow measurement—mechanical thrombectomy—near-infrared spectroscopy—diffuse correlation spectroscopy—ischemic stroke—recanalization

© 2019 Elsevier Inc. All rights reserved.

From the \*Institute of Physics, University of Campinas, Campinas, SP, Brazil; †Brazilian Institute of Neuroscience and Neurotechnology, Campinas, SP, Brazil; ‡Department of Physics & Astronomy, University of Pennsylvania, Philadelphia, Pennsylvania; §Department of Neurology, University of Pennsylvania, Philadelphia, Pennsylvania; ||Division of Neurology, Children's Hospital of Philadelphia, Philadelphia, Pennsylvania; ¶Department of Anesthesiology and Critical Care, University of Pennsylvania, Philadelphia, Pennsylvania; #Department of Neurosurgery, University of Pennsylvania, Philadelphia, Pennsylvania; and \*\*Department of Radiology, University of Pennsylvania, Philadelphia, Pennsylvania.

Received October 12, 2018; revision received February 28, 2019; accepted March 6, 2019.

Data were collected at the Hospital of the University of Pennsylvania.

Funding: National Institutes of Health (NIH) through grants R01-NS060653 (AGY), P41-EB015893 (AGY and JAD), and 1R01NS082309-01A1 (WK, RB, WB, and AY). Sao Paulo Research Foundation (FAPESP) through grants 2013/07559-3 (RCM) and 2016/13139-5 (RMF).

Address correspondence to Rodrigo M. Forti, MSc, Institute of Physics, University of Campinas, Rua Sérgio Buarque de Holanda, 777, Campinas, SP, 13083-859, Brazil. E-mail address: rforti@ifi.unicamp.br.

††These authors contributed equally to this work.

1052-3057/\$ - see front matter

© 2019 Elsevier Inc. All rights reserved.

<https://doi.org/10.1016/j.jstrokecerebrovasdis.2019.03.019>

## Introduction

Mechanical thrombectomy has revolutionized treatment of patients with acute ischemic stroke due to large vessel occlusion (LVO), by providing rapid restoration of blood flow to ischemic brain tissue.<sup>1,2</sup> Currently, procedural success for mechanical thrombectomy is defined by the degree of vessel recanalization visualized by angiography, most often using the modified Thrombolysis in Cerebral Infarction score (mTICI).<sup>3</sup> However, only about one-third of patients experience complete recanalization. The majority are left with some degree of residual cerebral hemodynamic impairment,<sup>1</sup> which in turn correlates with infarct growth and greater long-term disability.<sup>4</sup> Moreover, the degree of large artery recanalization, an anatomic structural observation, does not always reflect parenchymal cerebral blood flow (CBF),<sup>5-7</sup> and this physiological factor holds potential to better predict infarct volume,<sup>6</sup> clinical outcome,<sup>7</sup> and inform medical management strategies. Currently, there is no suitable tool to measure CBF during mechanical thrombectomy in real time, thus a continuous bedside monitor has potential to impact patient care.

Invasive monitors that measure brain parenchymal vascular physiology are available in neurointensive care settings.<sup>8</sup> These devices, however, typically only provide data from a single subcortical location. They are also impractical for hyperacute stroke due to both the time required to place them and the risk of tissue injury and/or hemorrhage, particularly in patients treated with intravenous thrombolysis or antithrombotic medications. Less invasive CT and MR perfusion techniques provide quantification of CBF, but these diagnostics require transport to an imaging suite, utilize exogenous contrast agents, and generally offer only snapshots in time. Noninvasive diffuse optical methods have limited depth penetration and spatial resolution, but they are attractive for patients with cerebrovascular disease because they enable continuous, bedside, transcranial monitoring of microvascular CBF, and cerebral oxy- and deoxy-hemoglobin concentrations.<sup>9-23</sup> The diffuse optical measurement of CBF has been previously validated against several other techniques, such as Arterial Spin Labelling-MRI,<sup>24</sup> Xenon CT,<sup>25</sup> transcranial Doppler ultrasound,<sup>12,26,27</sup> phase-encoded velocity mapping MRI,<sup>28</sup> and fluorescent microspheres.<sup>29</sup>

Transcranial optical monitoring during mechanical thrombectomy has also been carried out recently with commercial near-infrared spectroscopy (NIRS) instrumentation<sup>14,23</sup>; commercial NIRS provides information about blood oxygen saturation changes in tissues located beneath the probe. While encouraging, these studies only found small changes in oxygen saturation, and the results did not necessarily correlate with outcome. Importantly, in these studies, the commercial NIRS systems may not have offered the most sensitive measure of change in the context of recanalization. Specifically, commercial NIRS may

not accurately distinguish scalp and brain, and direct CBF monitoring with DCS, which is not possible with NIRS, may be a more sensitive tool for probing physiological changes during mechanical thrombectomy. The DCS blood flow signal is weighted toward comparatively long photon paths that penetrate more deeply into the brain (e.g., compared to NIRS).<sup>17,30</sup> Additionally, the relative difference between intracerebral and extracerebral blood flow is greater than the relative difference in oxygen saturation between these 2 compartments. Therefore, the present work anticipates that optical monitoring of CBF using DCS is inherently more sensitive to cerebral physiology changes than commercial NIRS systems.<sup>9,16,17,31,32</sup>

In this preliminary report, we describe findings using DCS to measure in real-time bilateral frontal lobe microvascular CBF during and after recanalization of the internal carotid artery (ICA) in 2 acute ischemic stroke patients. We focused on patients with ICA occlusion because the frontal lobes are reliably included in the ICA vascular distribution. This work documents important first steps toward establishing continuous diffuse optical monitoring of cerebral microvasculature as a means for noninvasive, patient-specific quantification of tissue-level reperfusion following mechanical thrombectomy.

## Methods

### *Patients*

Two patients undergoing mechanical thrombectomy to treat acute ischemic stroke caused by unilateral occlusion of the internal carotid artery (ICA) were enrolled in this study at the Hospital of the University of Pennsylvania. The study was carried out in accordance with the Belmont Report with written informed consent from all subjects (or legally authorized surrogate). Given the time-sensitive nature of mechanical thrombectomy and the nonsignificant risk associated with this research protocol, written informed consent was obtained retrospectively. The protocol was approved by the University of Pennsylvania Institutional Review Board (Protocol Number 828249).

### *Experimental Protocol*

Eligible patients were identified by a vascular neurologist. In accordance with standard-of-care, patients were transported to the interventional neuroradiology suite in order to perform mechanical thrombectomy. After the patient was situated on the procedure table, optical probes were placed bilaterally on the lateral aspect of the forehead (Fig 1). To optimize the optical signal, care was taken with probe placement to avoid hair and frontal sinuses. The probes were fixed to the head with double-sided tape and an elastic bandage. Once the probes were secured, the light sources were turned on, and cerebral hemodynamic data were collected throughout the course of the mechanical thrombectomy procedure. Briefly, the

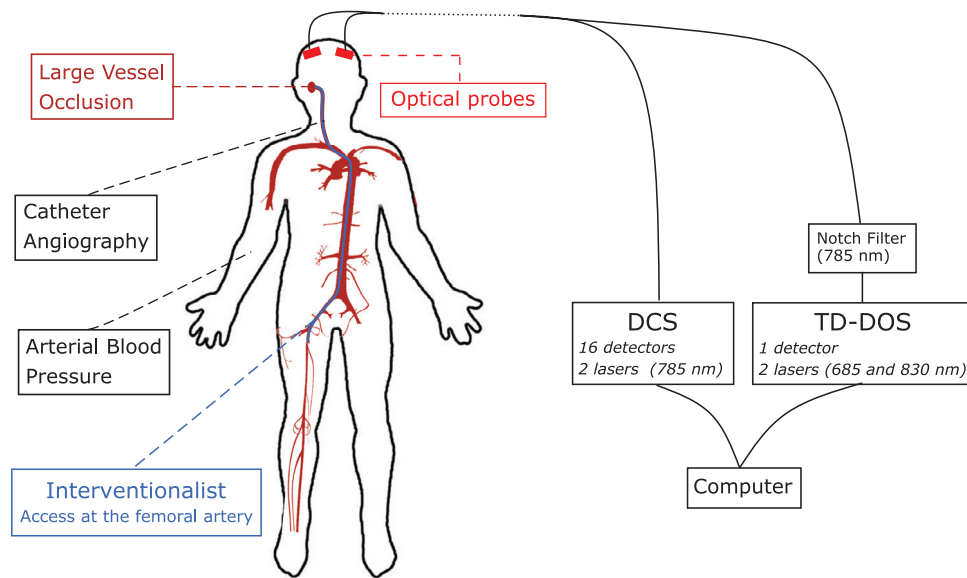


**Figure 1.** Schematic of the experimental setup. After the patient was situated on the procedure table, 2 fiberoptic optical monitoring probes were placed on the lateral aspect of the forehead, bilaterally. Groin access and mechanical thrombectomy proceeded without delay. Microvascular cerebral blood flow (CBF), oxyhemoglobin concentration, and deoxyhemoglobin concentration were simultaneously monitored on the ipsilateral hemisphere with diffuse correlation spectroscopy (DCS) and time-domain diffuse optical spectroscopy (TD-DOS). A notch filter (centered at 785 nm) was placed in front of the TD-DOS detector to facilitate simultaneous TD-DOS/DCS measurements. On the contralateral hemisphere, CBF alone was monitored with DCS.

mechanical thrombectomy procedure involves threading a catheter through the femoral artery to reach the clot in the cervicocerebral artery and then mechanically remove it.

Patients routinely remained on the procedure table for several minutes after completion of the thrombectomy, and optical data collection continued during this time. Just prior to removing the patient from the procedure table, data collection was stopped, and the optical probes were removed from the patient's head. An optical time-domain DOS (TD-DOS) instrument response function (IRF) measurement was then obtained in a manner described elsewhere.<sup>33</sup> Mean arterial pressure (MAP) data were recorded once every minute and were retrospectively retrieved from the anesthesia record and time-synchronized with the optical data. MAP was monitored either with an invasive catheter or a brachial cuff, depending on clinical availability.

### Optical Instrumentation

We utilized an instrument with TD-DOS and DCS modules. The TD-DOS module contains 2 pulsed lasers (BHLP-700, Becker&Hickl) emitting short light pulses (~100 ps) at a 50 MHz repetition rate and operating at different wavelengths (685 and 830 nm), 1 hybrid photomultiplier tube (HPM-100, Becker&Hickl), and a time-correlated single-photon counter board (SPC130, Becker&Hickl). The DCS system contains 16 single-photon counters (SPCM-AQ4C, Pacer) connected to a fast software correlator,<sup>34</sup> as well as 2 long-coherence-length

source lasers emitting light at 785 nm (DL785-100-SO, CrystaLaser).

To permit simultaneous TD-DOS/DCS measurements, we introduced a fiber-coupled notch filter centered at 785 nm before the TD-DOS detector; the notch filter blocks light from the DCS source (OZ Optics, Fig 1). Data acquisition was controlled with custom-written software in a LabVIEW environment (National Instruments). The data acquisition rate was 20 Hz for DCS and 0.7 Hz for TD-DOS (0.35 Hz per TD-DOS wavelength). For DCS, we employed 2 source-detector separations on each hemisphere: 1 short separation (0.7 cm) primarily sensitive to extracerebral tissue, that is, scalp and skull, and 1 long source-detector separation (2.5 cm), which has been shown to provide an acceptable signal-to-noise ratio (SNR) and cortical sensitivity.<sup>9,16,17,31</sup> Since we were limited to the use of a single TD-DOS detector, the TD-DOS measurement was made with a single, large source-detector separation (3.2 cm) on the hemisphere of interest, that is, ipsilateral to the occlusion. The TD-DOS technique, which is more complex than commercial NIRS systems that utilize continuous-wave light, can uniquely separate tissue absorption effects from tissue scattering effects for enhanced measurement accuracy.<sup>35</sup> For more details on DCS and TD-DOS instrumentation, we refer the reader to recent reviews.<sup>36-38</sup>

### Optical Analysis

The temporal decay of the DCS autocorrelation function and the recovered CBF indices are sensitive to the optical

properties of the underlying tissues. Thus, to improve DCS accuracy, we estimate the tissue absorption and reduced scattering coefficients independently with TD-DOS.<sup>39,40</sup> The TD-DOS technique measures the distribution of photon time-of-flight (DTOF) at each wavelength. The DTOF is a histogram of the number of photons striking the detector as a function of the time difference between source trigger and photon detection at time  $t$ . For each TD-DOS wavelength,  $\lambda$ , we fit the baseline-averaged DTOF (i.e., averaged over the  $\sim 5$ -minute interval before initiation of cerebral vasculature manipulation) to a convolution of the TD-DOS IRF and the semi-infinite Green's function solution of the photon diffusion equation. This procedure enables the calculation of baseline tissue absorption and reduced scattering coefficients, that is,  $\mu_{a,0}(\lambda)$  and  $\mu'_{s,0}(\lambda)$ , along with the effective launch time of the incident source pulse on the tissue ( $T_o$ ).<sup>36,41</sup> Thereafter, the DTOF acquired at every measurement time was fit to derive an absorption coefficient,  $\mu_a(\lambda)$ ; these fits assumed constant reduced scattering coefficient and constant  $T_o$  (both derived from the baseline fit). The multispectral tissue absorption measurements also assume a water volume fraction of 0.75. This scheme permits recovery of oxy- and deoxyhemoglobin concentration at every time-point.

This concentration information, in turn, enables calculation of the tissue absorption coefficient at the DCS wavelength (785 nm) using the chromophore extinction coefficients.<sup>42</sup> A multispectral model for tissue-reduced scattering coefficients (ie,  $\mu'_s(\lambda) = A\lambda^b$ ) was also employed in analyzing baseline measurements to obtain the  $A$  and  $b$  parameters; these parameters permit calculation of the baseline reduced scattering coefficient at the DCS wavelength (785 nm).<sup>42</sup> TD-DOS oxygenation results are shown in Supplemental Figure 1.

To help distinguish between intracerebral and extracerebral blood flow changes, we employed a multidistance DCS measurement. An *approximate* rule of thumb, which we will utilize in our thinking and analysis, is that the short source-detector separations measure extracerebral blood flow changes, while the long source-detector separations measure relative changes of cerebral blood flow (rCBF).

To improve the signal quality, we first down-sample the DCS data by averaging sequential sets of 2 temporal autocorrelation curves measured by DCS, for each source-detector separation. Then, to recover the blood flow changes, we separately fit the autocorrelation curves for each separation using a semi-infinite homogenous tissue model.<sup>35</sup> We use a baseline-averaged autocorrelation curve (averaged over  $\sim 5$  minutes before the initiation of cerebral vasculature manipulation) to determine the coherence factor in the Siegert relation ( $\beta$ ).<sup>43</sup> Next, we fit every frame for the DCS blood flow index, assuming that  $\beta$  remains constant throughout the procedure. Finally, to reduce the effects of systemic physiological variations, the data were low-pass

filtered using a Butterworth filter with a cut-off frequency of 0.0167 Hz. All analysis scripts were written using open-source libraries based on Python 3.6.<sup>44-46</sup>

## Results

Between December 1, 2017 and July 2, 2018, 2 patients with ICA occlusion were studied as part of a broader ongoing protocol evaluating the safety and efficacy of transcranial optical monitoring during mechanical thrombectomy. Since we were restricted to measurements on the forehead in this study, and since measurements on the forehead may not be sensitive to all MCA occlusions, herein we focus on and describe only preliminary results from the 2 ICA occlusion patients. In both cases, mechanical thrombectomy was performed under general anesthesia. Endotracheal intubation occurred immediately prior to the initiation of optical monitoring, and mechanical ventilation continued throughout the course of the monitoring protocol.

Patient 1 presented with acute onset aphasia and right hemiplegia, with admission NIH stroke scale (NIHSS) of 24. She was not eligible for intravenous thrombolysis because of oral anticoagulation use. She was transferred for consideration of mechanical thrombectomy; initial imaging revealed left ICA occlusion with patent intracranial circulation. Left hemisphere appeared to be filling via the anterior communicating artery. CT perfusion identified a large territory at risk of infarction. While CTA suggested a cervical ICA occlusion, catheter angiogram identified the occlusion in the intracranial ICA segment. Slow proximal flow created the false appearance of a more proximal occlusion on noninvasive imaging. Successful recanalization (mTICI 2B) was achieved with a single pass of a Solitaire stent retriever (Medtronic PLC). Table 1 summarizes the patient's clinical details. Figure 2 shows relevant neuroimaging studies, that is, CT perfusion/structural images and angiograms, before and after mechanical thrombectomy, and we present the end-tidal CO<sub>2</sub> and anesthesia doses in Supplemental Figure 2. For this patient, MAP was recorded noninvasively at the beginning of the procedure, but eventually, an invasive catheter was inserted (radial artery) for continuous blood pressure monitoring during a portion of the procedure.

At the time of recanalization, a large increase in optically measured rCBF was observed in the affected hemisphere, with *minimal change* in extracerebral blood flow (Fig 3A). After recanalization, despite a large MAP fluctuation (from 64 to 110 mm Hg), CBF remained elevated, which could reflect intact autoregulatory mechanisms in the reperfused cerebral tissue. In the contralateral hemisphere, we also observed a transient increase in CBF at the time of recanalization, but it returned to baseline after a few minutes (Fig 3B).

No complications occurred during mechanical thrombectomy. Patient 1 experienced near complete resolution

**Table 1.** Baseline, procedural, and outcome summary

	Patient 1	Patient 2
Baseline		
Age	80-85	60-65
NIHSS	24	15
Vessel occlusion	Left cervical ICA	Right cervical ICA
ASPECTS	8	7
Infarct core (cc)*	5	19
Penumbra (cc)*	187	97
Procedural details		
Time from onset to recanalization (min)	196	278
Final mTICI score	2B	2B
early complications	None	Difficulty achieving revascularization in context of ICA dissection
Late complications	None	Edema and hemorrhagic conversion necessitating decompressive hemicraniectomy
Outcome		
Discharge NIHSS	1	17
Discharge disposition	Home	Rehab

\*Based on CT perfusion imaging analysis by RAPID software (iSchemaView, Inc. Redwood City, CA). Infarct core is defined by CBF < 30%. Penumbra is defined by  $T_{max} > 6$  seconds.

of her neurologic deficits, and she was discharged on hospital day 5 with an NIHSS of 1.

Patient 2 experienced several episodes of emesis and retching in the context of presumed gastroenteritis.

Less than an hour following an episode of retching, she developed severe right-sided neck pain followed by acute onset left hemiplegia. She presented with an NIHSS of 15 to her local emergency room. She was treated with

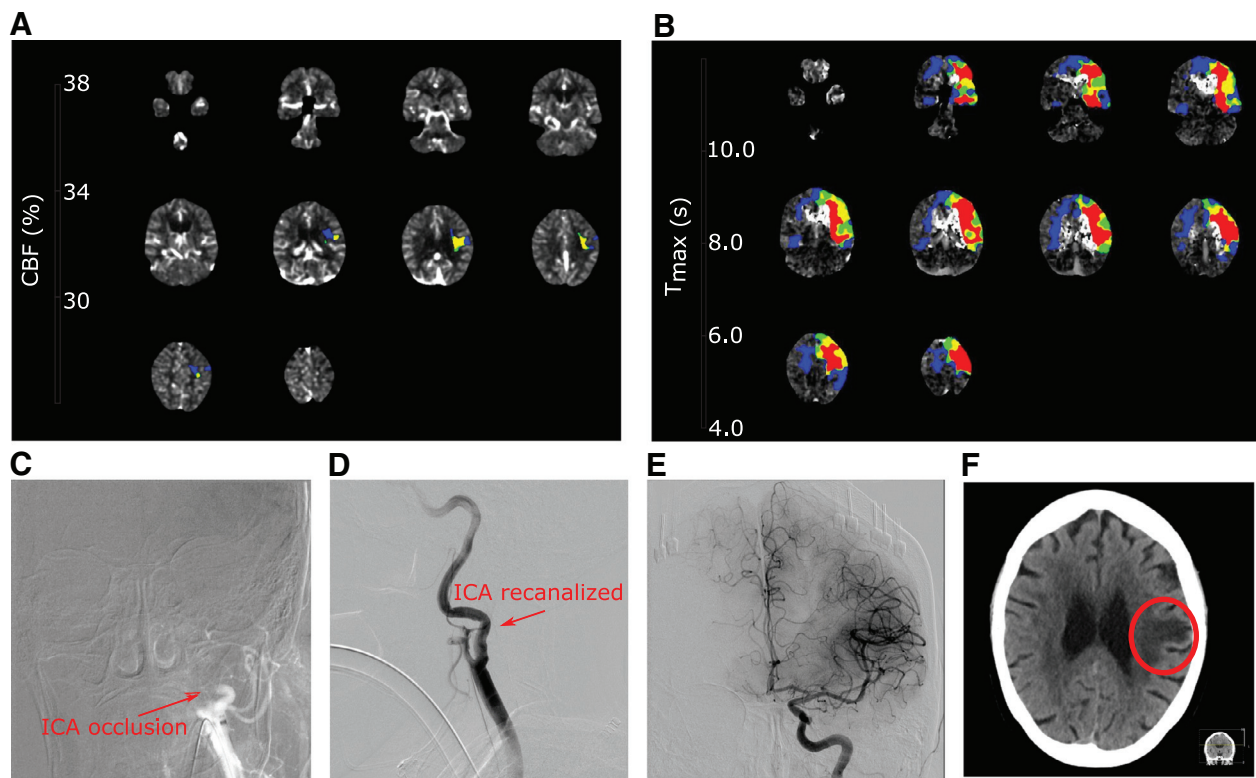


**Figure 2.** Imaging before and after mechanical thrombectomy (Patient 1). Baseline CT perfusion as analyzed by RAPID software (iSchemaView, Inc. Redwood City, CA) indicates (A) a small infarct core in the left hemisphere, as defined by cerebral blood flow (CBF) lower than 30% of the contralateral values, and (B) a large penumbra, as defined by regions where the time to maximum ( $T_{max}$ ) of the residue function obtained by deconvolution is higher than 6 s. (C) Angiogram confirmed patency of the left common carotid artery and occlusion of the internal carotid artery (ICA). After mechanical thrombectomy, an angiogram revealed (D) ICA recanalization, as well as (E) patent intracranial circulation. (F) Follow-up CT identified a small left lateral frontal lobe infarction (red circle).

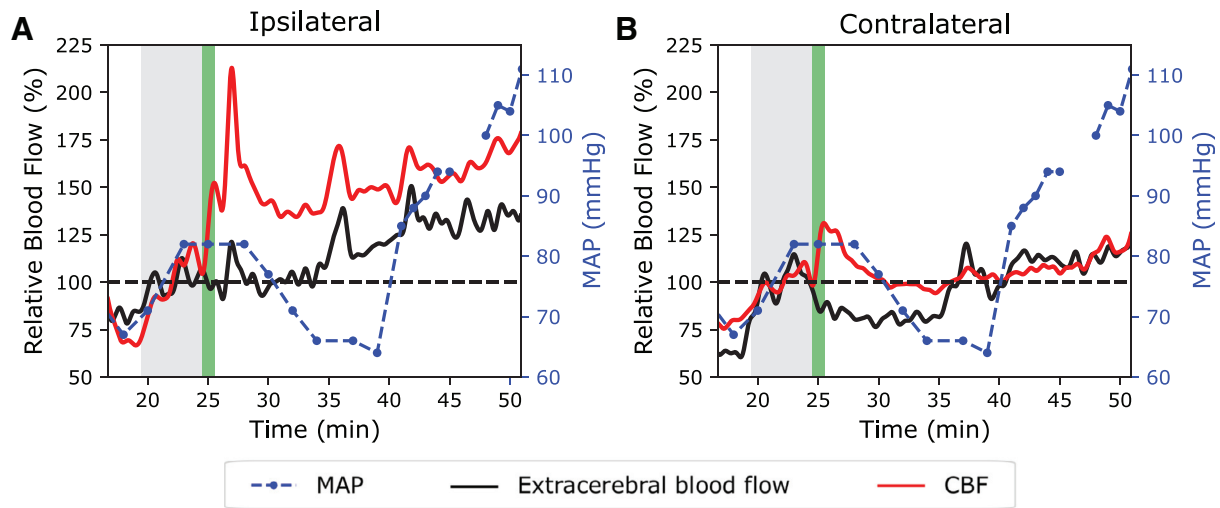


**Figure 3.** Hemodynamics of recanalization (Patient 1). Optical flow monitoring revealed a large and sudden increase in (A) ipsilateral CBF (red solid line, left axis) after recanalization (green bar); this sudden increase was not mimicked by the extracerebral tissue, which instead showed minimal blood flow changes at these times (black solid line, left axis). We also observed a smaller transient (B) contralateral CBF increase. Despite MAP fluctuations (blue dashed line, right axis), after recanalization CBF remained relatively stable on both sides. The grey-shaded region represents the baseline period.

intravenous thrombolysis and was transferred for consideration of mechanical thrombectomy. Upon arrival, her neurologic deficit was unchanged, and imaging revealed right cervical ICA occlusion with intact intracranial

vasculature. Right hemisphere appeared to be filling via the anterior communicating artery. Her clinical details are summarized in [Table 1](#), while the end-tidal CO<sub>2</sub> changes and anesthesia doses are presented in

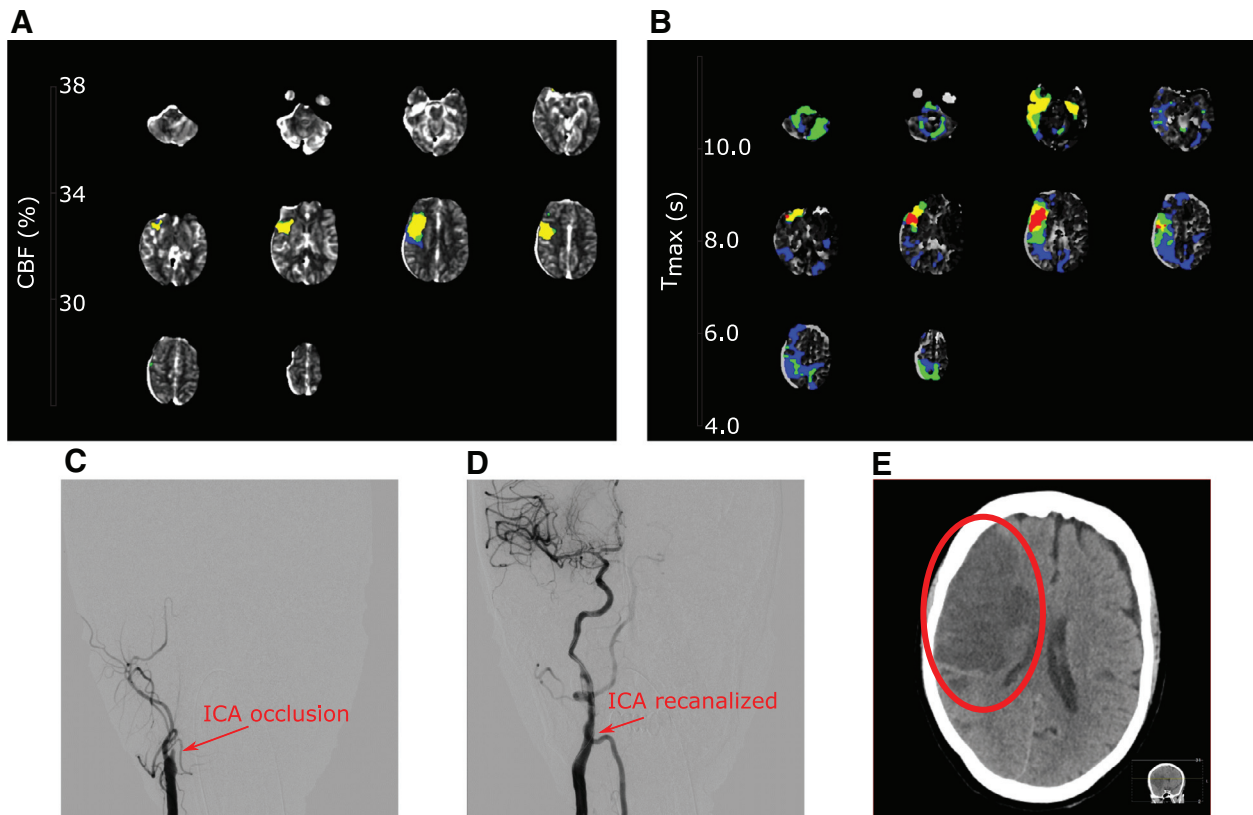


**Figure 4.** Imaging before and after mechanical thrombectomy (Patient 2). Baseline CT perfusion as analyzed by RAPID software (iSchemaView, Inc. Redwood City, CA) indicates (A) small-to-moderate infarct core in the right hemisphere, as defined by cerebral blood flow (CBF) lower than 30% of the contralateral values, and (B) large penumbra, as defined by regions where the time to maximum ( $T_{max}$ ) of the residue function obtained by deconvolution is higher than 6 s. (C) Angiogram confirmed right cervical ICA occlusion, which was ultimately (D) recanalized after stent placement. (E) Follow-up CT identified a very large right hemispheric infarction (red circle).

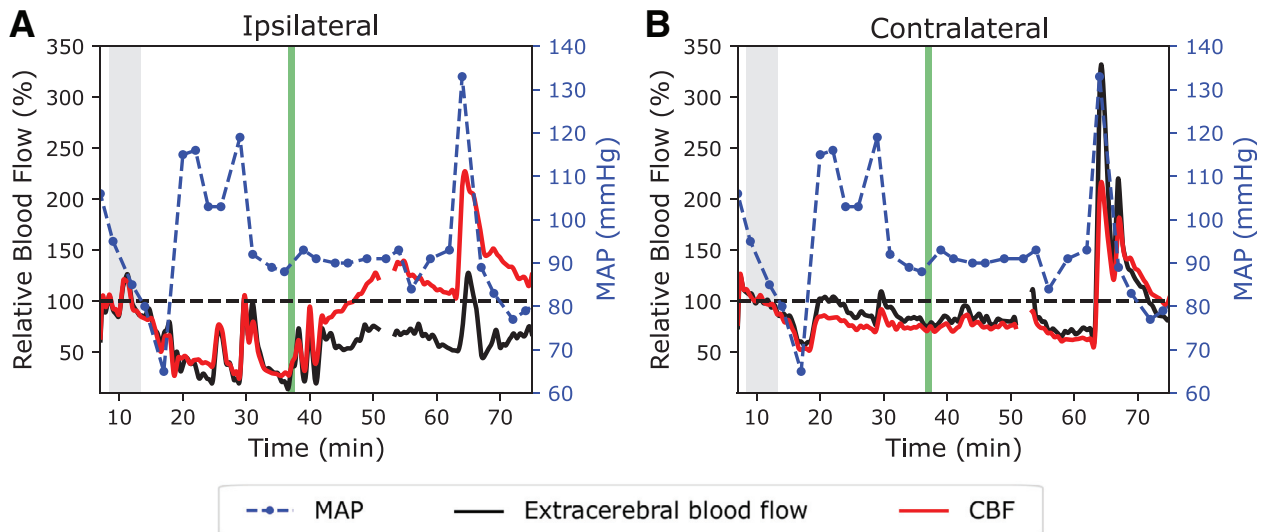


**Figure 5.** Hemodynamics of recanalization (Patient 2). Optics revealed a large and gradual increase in (A) ipsilateral CBF (red solid line, left axis) after recanalization (green bar), with minimal (B) contralateral CBF and extracerebral blood flow (black solid line, left axis) changes (black solid line, left axis). Prior to recanalization, a large drop in MAP (blue dashed line, right axis) was accompanied by a bilateral decrease ( $\sim 50\%$ ) in CBF and extracerebral flow. Blood pressure was augmented pharmacologically, which resulted in an increase in contralateral flow but failed to improve flow on the side of the occlusion. The grey-shaded region represents the baseline period.

Supplemental Figure 3. Radiological imaging is presented in Figure 4. For this patient, MAP was noninvasively monitored by brachial cuff throughout the protocol. The decision was made to proceed with mechanical thrombectomy. Because of ICA dissection and associated occlusion, the ICA was difficult to traverse, and after multiple attempts at angioplasty, an ICA stent was ultimately placed. There was no evidence of intracranial occlusion. When the ICA was first manipulated, there was a steep decline in MAP (124 to 66 mm Hg), which was likely a consequence of carotid sinus disruption. This decline in MAP was accompanied by a bilateral decrease ( $\sim 50\%$ ) in CBF and extracerebral flow (Fig 5). Blood pressure was then augmented pharmacologically; this increased contralateral flow but failed to improve blood flow on the side of the occlusion. Over the subsequent 15 minutes (prior to successful stent placement), blood flow in the affected hemisphere fluctuated dramatically.

More detailed inspection revealed that at times of low CBF, a near-total loss of pulsatile flow is occurred, along with intermittent periods of flow restoration. Even with stable MAP on pressors, pulsatile flow in Patient 2 was not always maintained (Fig 6). At the time of stent placement, ipsilateral CBF continued to fluctuate for several minutes and slowly increased to almost 50% above the baseline value, despite stable MAP. Another spike in MAP was accompanied by a large CBF spike to almost double the baseline value. Notably, the intermittent loss of pulsatile flow was only seen in the ipsilateral CBF and was first instigated by the significant decrease in MAP prior to recanalization (Figs 5 and 6).

Immediate follow-up head CT showed evolved right hemispheric infarction along with patchy hyperdensity throughout the hemisphere. This is suggestive of a combination of contrast extravasation and some component of hemorrhage. The patient's final infarct burden was very large, with associated edema and mass effect, necessitating decompressive hemicraniectomy on hospital day 3. She was eventually discharged to a rehabilitation facility on hospital day 24, with an NIHSS of 17.

## Discussion

In this proof-of-concept study, we employed a noninvasive, contrast-free optical technique to monitor frontal lobe hemodynamics at the bedside during mechanical thrombectomy. To help distinguish between extracerebral and intracerebral blood flow changes, we obtained data from short (0.7 cm) and long (2.5 cm) source-detector separations. In 2 patients with ICA occlusion, we measured an increase in ipsilateral CBF after recanalization while detecting no significant changes in extracerebral flow. A detailed inspection of the CBF temporal response to mechanical thrombectomy revealed 2 distinct hemodynamic responses associated with divergent clinical outcomes. Note, the DCS signal has contributions from arterial, capillary, and venous compartments. If cerebral blood volume is not transiently changing, the total blood flow in each vascular compartment is equal, and the precise compartmental contributions will not influence the measurement. When blood volume is transiently changing, DCS is more sensitive to arterial contributions.<sup>26,47</sup>

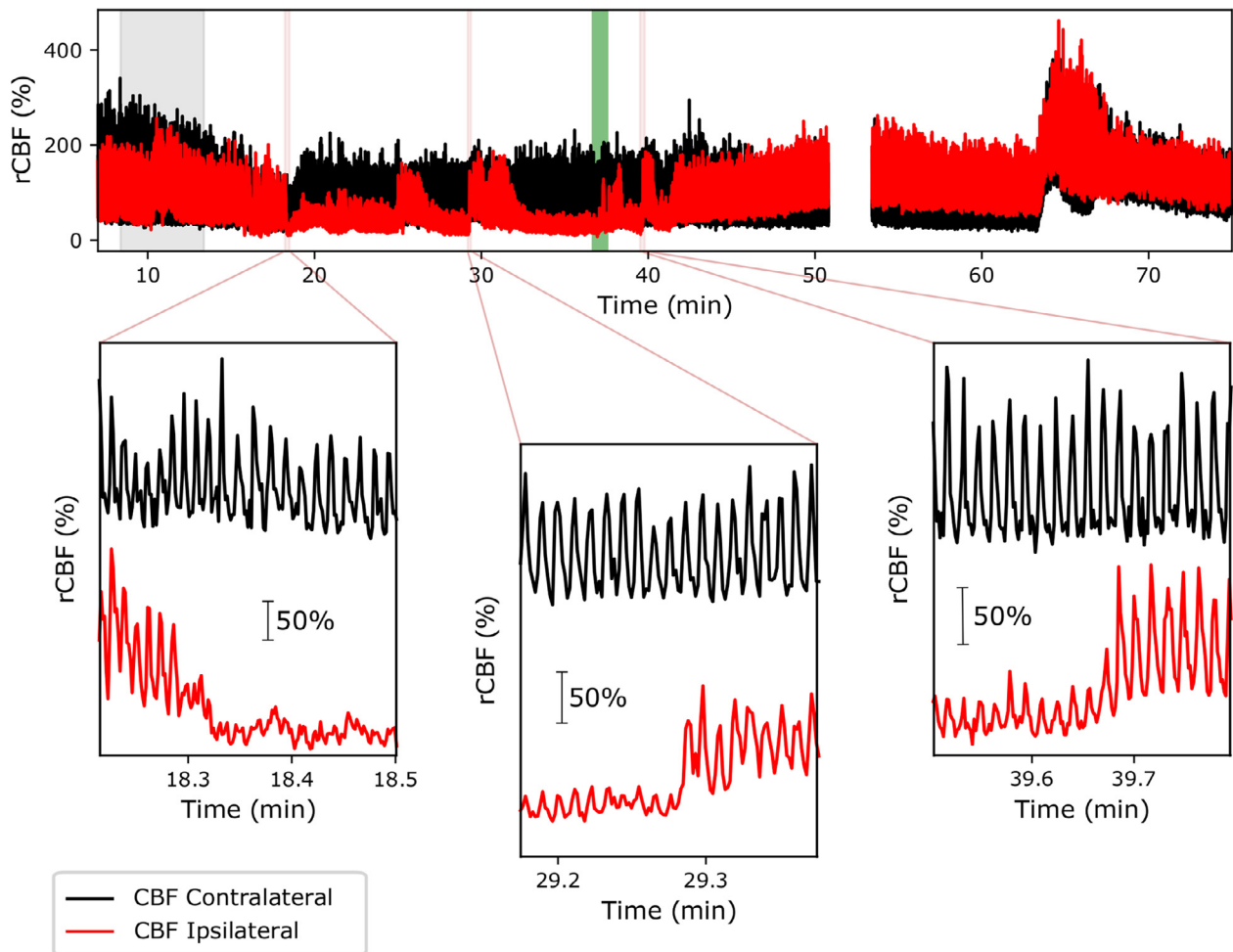


**Figure 6.** Ipsilateral (red) and contralateral (black) CBF changes from Patient 2, before filtering. The top panel shows CBF changes throughout the procedure. The green bar indicates the time of recanalization, and the grey-shaded region indicates the baseline period. Each of the 3 bottom panels exhibit fast (without filtering) time variation in 1 of the 3 red-shaded regions. These scaled zoomed-in versions of ipsilateral and contralateral CBF were separated to show the difference in heart-rate pulsatility across the different hemispheres and time.

Patient 1 experienced a large and sudden increase in CBF after recanalization, which was sustained over the remainder of the monitoring period (~25 min). Notably, after recanalization, CBF remained elevated despite a large MAP fluctuation (between 64 and 111 mm Hg), perhaps reflecting intact cerebrovascular autoregulation. Although it is often assumed that stroke impairs autoregulation,<sup>48</sup> this assumption may not be true for all brain regions or for all patients,<sup>49</sup> and may be affected by anesthetic drug and procedure factors.<sup>50</sup> In Patient 1, the large and sustained increase in CBF, and the apparent intact autoregulation, likely reflects the hemodynamics of effectively salvaged tissue. In fact, in a short interval follow-up, this patient made a quick and near-complete recovery with a very small final infarct burden. This result suggests that continuous monitoring of CBF with diffuse optics may facilitate individualized blood pressure goals aimed at optimizing CBF.

Interestingly, at the time of ICA recanalization in Patient 1, a transient increase in contralateral CBF was also observed. Prior to recanalization, this patient was

perfusing the left hemisphere via the right carotid system with right-to-left flow through a patent anterior communicating artery. It is conceivable that this creates a “steal” phenomenon, in which blood flow to the unaffected right hemisphere is reduced. After recanalization, right-to-left flow through the anterior communicating artery is reduced and CBF in the right hemisphere increases. Additionally, some of this change could be related to MAP, which was elevated around the time of recanalization, and subsequently decreased ~5 minutes following recanalization.

In Patient 2, we observed a more gradual increase in CBF after recanalization, along with an intermittent loss of pulsatile flow, i.e., as seen by our fast DCS module on the ipsilateral hemisphere, but not the contralateral hemisphere (Fig 6). In fact, the initial loss of pulsatile flow coincided with a decline in MAP. These observations may indicate microvascular collapse in a low-flow state, perhaps enhanced by early infarct-related edema or elevated vasomotor tone of smooth muscle in arterioles.<sup>26</sup>

Interestingly, with MAP augmentation, there was intermittent restitution of pulsatile flow. However, pulsatile flow was not well sustained, and even with ICA recanalization, we did not detect sudden increases in CBF, perhaps reflective of persistent microvascular dysfunction. These observations highlight another potentially valuable application of these bedside optics, that is, in cases wherein the angiographic appearance of large vessel recanalization fails to adequately describe the hemodynamic state of the tissue. Identification of microvascular impairment after recanalization could enable clinicians to identify patients experiencing “no-reflow,” which has long been a nebulous and challenging clinical phenomenon that is associated with morbidity and mortality.<sup>51,52</sup>

In the case of Patient 2, the microvascular perturbation occurred in a patient that ultimately suffered a very large infarction. It is not clear if the microvascular impairment led to infarct expansion, or if the flow impairment was a consequence of the developing infarction. The temporal relationship of CBF with hypotension supports the former hypothesis, but conclusions should not be drawn from a single case. Ongoing studies will help to define the incidence of this discordance between large artery and microvascular flow and may identify additional hemodynamic patterns that occur with recanalization. Ultimately, the ability to noninvasively assess tissue reperfusion before and after recanalization may aid clinicians to more quickly assess treatment efficacy and concurrent physiologic management, such as blood pressure goals and head of bed angle.

It is also important to note that Patient 2 only achieved recanalization after extensive ICA manipulation, including multiple angioplasty attempts, and eventual ICA stenting. Some of the fluctuations before recanalization may reflect transient flow changes after balloon angioplasty, but we could not reliably synchronize the optical signal with every endovascular manipulation. In future studies, care will need to be taken to document endovascular manipulation in detail, as this may influence CBF or, equally important, may confirm that the hemodynamic changes are independent of endovascular manipulation. In this initial feasibility study, monitoring was limited to the interventional radiology suite, but continued monitoring in the ICU may present opportunities to further characterize post-recanalization stroke physiology in future work.

Variations in anesthetic depth impact cerebral metabolism and possibly influence outcome,<sup>53,54</sup> although clear clinical evidence of neuroprotection from anesthetics in cerebral ischemia has proven elusive.<sup>55</sup> Unfortunately, we could not determine anesthetic depth due to a lack of EEG monitoring during the procedure. The anesthetic dose was abstracted from the anesthesia record, but it only crudely approximates the depth of anesthesia. Furthermore, it is challenging to draw any conclusions regarding the impact of cerebral metabolism changes due, in part, to limitations of steady-state modeling. Notably, both

anesthesia and evolving ischemic conditions influence cellular metabolism, neither of which are static variables. Nevertheless, the observed sudden asymmetric changes in flow are not likely the effect of anesthesia, since the anesthesia effects would likely be more diffuse.

One current limitation of DCS is that hair can disrupt the DCS signal and delay probe placement; thus, measurements in this study were restricted to the anterior frontal lobe. Given this limitation, care was taken to place the probes on the lateral aspect of the forehead. In this position, diffuse optics likely measures a combination of ACA and MCA flow, rather than exclusively MCA flow. This situation presents less of a problem for patients with ICA occlusion, but it may be an important consideration when monitoring patients with MCA occlusion in whom we expect reduced sensitivity to parenchymal changes. CT perfusion imaging that is now routinely obtained in acute stroke patients may help identify patients in whom flow impairment can be detected using frontally placed optical probes. Ultimately, with more reliable and rapid DCS systems capable of transcranial monitoring through hair, more targeted placement of the optical probes over tissues of primary interest will be possible.

Another limitation of our study is the use of a semi-infinite homogenous medium tissue model for light transport, which may underestimate CBF changes.<sup>9,16,17,31,56</sup> Furthermore, light detected by the long source-detector separation is also sensitive to extracerebral changes, as these photons traverse the extracerebral tissues before reaching the intracerebral tissues. This could lead to an erroneous interpretation of extracerebral blood flow changes as CBF changes. Nonetheless, by using multidistance measurements, our results demonstrated that mechanical thrombectomy primarily affected CBF, as measured by the long source-detector separation, which is consistent with the underlying vascular anatomy and supports the notion that long DCS source-detector separations are primarily affected by cerebral tissue. In future studies, multilayer approaches for DCS/DOS can and should be used to more carefully separate intracerebral and extracerebral blood flow changes.<sup>56-63</sup> Calibration of CBF indices recovered from DCS would enable absolute comparison of CBF across subjects,<sup>39,64</sup> but this is unlikely to affect the relative flow reported in this study.

## Conclusions

We have demonstrated the feasibility of real-time monitoring of cerebral flow hemodynamics during mechanical thrombectomy. By measuring the frontal lobe microvascular hemodynamics with diffuse optics, it was possible to observe distinct perfusion profiles in 2 patients with divergent clinical outcomes. Although future studies in larger populations are clearly needed to better delineate application opportunities for DCS/DOS optical hemodynamic monitoring during mechanical thrombectomy, this pilot demonstration of diffuse optics shows promise for

assessing the response to endovascular treatment and for guiding physiology-based therapy in this and other contexts.

### Acknowledgments

We acknowledge the support of the National Institute of Health (NIH) through grants R01-NS060653 (AY), P41-EB015893 (AY and JD), and 1R01NS082309-01A1 (WK, RB, WB, and AY), as well as the support by the Sao Paulo Research Foundation (FAPESP) through grants 2013/07559-3 (RM) and 2016/13139-5 (RF). We would also like to acknowledge the research coordinator responsible for this project, Nichole Galatti.

### Conflict of Interest

AY and JD are inventors on USA Patent #8082015, "Optical measurement of tissue blood flow hemodynamics and oxygenation." Several authors (AY, JD, WK, WB, RB and RM) are also inventors on pending patent applications for associated DCS technologies. No compensation for this intellectual property has been received by any author, the University of Pennsylvania or the University of Campinas.

### Author Contributions

RF and CF collected all the data and wrote the first draft of the manuscript. RF, JC, WB, RM, and AY designed the data analysis protocol, and RF conducted the final analysis. DK, NS, BP, RH, and OC performed the endovascular treatments described. All authors assisted with data interpretation, contributed to manuscript revision, read and approved the submitted version.

### Supplementary Materials

Supplementary data to this article can be found online at doi:[10.1016/j.jstrokecerebrovasdis.2019.03.019](https://doi.org/10.1016/j.jstrokecerebrovasdis.2019.03.019).

### References

- Goyal M, Menon BK, Van Zwam WH, et al. Endovascular thrombectomy after large-vessel ischaemic stroke: a meta-analysis of individual patient data from five randomised trials. *Lancet* 2016;387:1723-1731.
- Powers WJ, Rabinstein AA, Ackerson T, et al. 2018 Guidelines for the early management of patients with acute ischemic stroke: a guideline for healthcare professionals from the American Heart Association/American Stroke Association. *Stroke* 2018;49:e46-e49. <https://doi.org/10.1161/STR.0000000000000158>.
- Zaidat OO, Yoo AJ, Khatri P, et al. Recommendations on angiographic revascularization grading standards for acute ischemic stroke: a consensus statement. *Stroke* 2013;44:2650-2663. <https://doi.org/10.1161/STROKEAHA.113.001972>.
- Chamorro Á, Blasco J, López A, et al. Complete reperfusion is required for maximal benefits of mechanical thrombectomy in stroke patients. *Sci Rep* 2017;7:11636. <https://doi.org/10.1038/s41598-017-11946-y>.
- Tomsick T. Long-term clinical follow-up of therapeutic internal carotid artery occlusion. *Am J Neuroradiol* 2007;28:1626.
- Soares BP, Tong E, Hom J, et al. Reperfusion is a more accurate predictor of follow-up infarct volume than recanalization: a proof of concept using CT in acute ischemic stroke patients. *Stroke* 2010;41:34-41.
- Eilaghi A, Brooks J, d'Estre C, et al. Reperfusion is a stronger predictor of good clinical outcome than recanalization in ischemic stroke. *Radiology* 2013;269:240-248.
- Le Roux P, Menon DK, Citerio G, et al. Consensus summary statement of the international multidisciplinary consensus conference on multimodality monitoring in neurocritical care. *Intensive Care Med* 2014;40:1189-1209. <https://doi.org/10.1007/s00134-014-3369-6>.
- Durduran T, Yodh AG. Diffuse correlation spectroscopy for non-invasive, micro-vascular cerebral blood flow measurement. *Neuroimage* 2014;85:5163.
- Kim MN, Edlow BL, Durduran T, et al. Continuous optical monitoring of cerebral hemodynamics during head-of-bed manipulation in brain-injured adults. *Neurocrit Care* 2014;20:443-453.
- Favilla CG, Parthasarathy AB, Detre JA, et al. Non-invasive respiratory impedance enhances cerebral perfusion in healthy adults. *Front Neurol* 2017;8:45.
- Parthasarathy AB, Gannon KP, Baker WB, et al. Dynamic autoregulation of cerebral blood flow measured non-invasively with fast diffuse correlation spectroscopy. *J Cereb Blood Flow Metab* 2017;38:230-240. <https://doi.org/10.1177/0271678X17747833>.
- Buckley EM, Parthasarathy AB, Grant PE, et al. Diffuse correlation spectroscopy for measurement of cerebral blood flow: future prospects. *Neurophotonics* 2014;1:011009.
- Ritzenthaler T, Cho TH, Mechtouff L, et al. Cerebral near-infrared spectroscopy a potential approach for thrombectomy monitoring. *Stroke* 2017;48:3390-3392.
- Favilla CG, Mesquita RC, Mullen M, et al. Optical bedside monitoring of cerebral blood flow in acute ischemic stroke patients during head-of-bed manipulation. *Stroke* 2014;45:1269-1274.
- Mesquita RC, Durduran T, Yu G, et al. Direct measurement of tissue blood flow and metabolism with diffuse optics. *Philos Trans R Soc A Math Phys Eng Sci* 2011;369:4390-4406.
- Selb J, Boas DA, Chan S-T, et al. Sensitivity of near-infrared spectroscopy and diffuse correlation spectroscopy to brain hemodynamics: simulations and experimental findings during hypercapnia. *Neurophotonics* 2014;1:015005.
- Muehlschlegel S, Selb J, Patel M, et al. Feasibility of NIRS in the neurointensive care unit: a pilot study in stroke using physiological oscillations. *Neurocrit Care* 2009;11:288-295.
- Pennekamp CWA, Immink RV, Den Ruijter HM, et al. Near-infrared spectroscopy can predict the onset of cerebral hyperperfusion syndrome after carotid endarterectomy. *Cerebrovasc Dis* 2012;34:314-321.
- Pennekamp CWA, Bots ML, Kappelle LJ, et al. The value of near-infrared spectroscopy measured cerebral oximetry during carotid endarterectomy in perioperative stroke prevention. A review. *Eur J Vasc Endovasc Surg* 2009;38:539-545.
- Shang Y, Cheng R, Dong L, et al. Cerebral monitoring during carotid endarterectomy using near-infrared

- diffuse optical spectroscopies and electroencephalogram. *Phys Med Biol* 2011;56:3015-3032.
22. Delgado-Mederos R, Gregori-Pla C, Zirak P, et al. Transcranial diffuse optical assessment of the microvascular reperfusion after thrombolysis for acute ischemic stroke. *Biomed Opt Express* 2018;9:1262.
  23. Hametner C, Stanarcevic P, Stampfl S, et al. Noninvasive cerebral oximetry during endovascular therapy for acute ischemic stroke: an observational study. *J Cereb Blood Flow Metab* 2015;35:1722-1728.
  24. Yu G, Floyd TF, Durduran T, et al. Validation of diffuse correlation spectroscopy for muscle blood flow with concurrent arterial spin labeled perfusion MRI. *Opt Express* 2007;15:1064-1075.
  25. Kim MN, Durduran T, Frangos S, et al. Noninvasive measurement of cerebral blood flow and blood oxygenation using near-infrared and diffuse correlation spectroscopies in critically brain-injured adults. *Neurocrit Care* 2010;12:173-180.
  26. Baker WB, Parthasarathy AB, Gannon KP, et al. Noninvasive optical monitoring of critical closing pressure and arteriole compliance in human subjects. *J Cereb Blood Flow Metab* 2017;37:2691-2705.
  27. Zirak P, Delgado-Mederos R, Martí-Fàbregas J, et al. Effects of acetazolamide on the micro- and macro-vascular cerebral hemodynamics: a diffuse optical and transcranial Doppler ultrasound study. *Biomed Opt Express* 2010;1:1443-1459.
  28. Buckley EM, Hance D, Pawlowski T, et al. Validation of diffuse correlation spectroscopic measurement of cerebral blood flow using phase-encoded velocity mapping magnetic resonance imaging. *J Biomed Opt* 2012;17:037007.
  29. Zhou C, Eucker SA, Durduran T, et al. Diffuse optical monitoring of hemodynamic changes in piglet brain with closed head injury. *J Biomed Opt* 2009;14:034015.
  30. Middleton AA, Fisher DS. Discrete scatterers and auto-correlations of multiply scattered light. *Phys Rev B* 1991;43:5934-5938.
  31. Durduran T, Yu G, Burnett MG, et al. Diffuse optical measurement of blood flow, blood oxygenation, and metabolism in a human brain during sensorimotor cortex activation. *Opt Lett* 2004;29:1766.
  32. Mesquita RC, Schenkel SS, Minkoff DL, et al. Influence of probe pressure on the diffuse correlation spectroscopy blood flow signal: extra-cerebral contributions. *Biomed Opt Express* 2013;4:978.
  33. Liebert A, Wabnitz H, Grosenick D, et al. Fiber dispersion in time domain measurements compromising the accuracy of determination of optical properties of strongly scattering media. *J Biomed Opt* 2003;8:512-516.
  34. Wang D, Parthasarathy AB, Baker WB, et al. Fast blood flow monitoring in deep tissues with real-time software correlators. *Biomed Opt Express* 2016;7:776.
  35. Durduran T, Choe R, Baker WB, et al. Diffuse optics for tissue monitoring and tomography. *Reports Prog Phys* 2010;73:076701.
  36. Torricelli A, Contini D, Pifferi A, et al. Time domain functional NIRS imaging for human brain mapping. *Neuroimage* 2014;85:28-50.
  37. Pifferi A, Contini D, Mora AD, et al. New frontiers in time-domain diffuse optics, a review. *J Biomed Opt* 2016: 21.
  38. Shang Y, Li T, Yu G. Clinical applications of near-infrared diffuse correlation spectroscopy and tomography for tissue blood flow monitoring and imaging. *Physiol Meas* 2017;38:R1-R26.
  39. Diop M, Verdecchia K, Lee T-Y, et al. Calibration of diffuse correlation spectroscopy with a time-resolved near-infrared technique to yield absolute cerebral blood flow measurements. *Biomed Opt Express* 2011;2:2068-2081.
  40. Irwin D, Dong L, Shang Y, et al. Influences of tissue absorption and scattering on diffuse correlation spectroscopy blood flow measurements. *Biomed Opt Express* 2011;2:1969-1985.
  41. Spinelli L, Martelli F, Farina A, et al. Accuracy of the non-linear fitting procedure for time-resolved measurements on diffusive phantoms at NIR wavelengths. *Proc SPIE* 2009:717424.
  42. Jacques SL. Optical properties of biological tissues: a review. *Phys Med Biol* 2013;58:R37-R61.
  43. Lemieux PA, Durian DJ. Investigating non-Gaussian scattering processes by using nth-order intensity correlation functions. *J Opt Soc Am A* 1999;16:1651-1664.
  44. Newville M, Stensitzki T, Allen DB, et al. LMFIT: non-linear least-square minimization and curve-fitting for python. *Zenodo* 2014. <https://doi.org/10.5281/zenodo.11813>.
  45. Oliphant TE. Python for Scientific Computing. *Comput Sci Eng* 2007: 10-20. <https://doi.org/10.1109/MCSE.2007.58>.
  46. Hunter JD. Matplotlib: a 2D graphics environment. *Comput Sci Eng* 2007;9:90-95. <https://doi.org/10.1109/MCSE.2007.55>.
  47. Boas DA, Sakadzic S, Selb J, et al. Establishing the diffuse correlation spectroscopy signal relationship with blood flow. *Neurophotonics* 2016;3:031412.
  48. Dawson SL, Panerai RB, Potter JF. Serial changes in static and dynamic cerebral autoregulation after acute ischaemic stroke. *Cerebrovasc Dis* 2003;16:69-75.
  49. Jordan JD, Powers WJ. Cerebral autoregulation and acute ischemic stroke. *Am J Hypertens* 2012;25:946-950.
  50. Kofke WA, Dong ML, Bloom M, et al. Transcranial Doppler ultrasonography with induction of anesthesia for neurosurgery. *J Neurosurg Anesthesiol* 1994;6:89-97.
  51. Soares BP, Chien JD, Wintermark M. MR and CT monitoring of recanalization, reperfusion, and penumbra salvage: everything that recanalizes does not necessarily reperfuse!. *Stroke* 2009;40:24-28.
  52. Dalkara T, Arsava E. Can restoring incomplete microcirculatory reperfusion improve stroke outcome after thrombolysis. *J Cereb Blood Flow Metab* 2012;32:2091-2099. <https://doi.org/10.1038/jcbfm.2012.139>.
  53. Stullken Edward H, Milde JH, Michenfelder John D, et al. The nonlinear responses of cerebral metabolism to low concentrations of halothane, enflurane, isoflurane, and thiopental. *Anesthesiol J Am Soc Anesthesiol* 1977;46:28-34.
  54. Nellgard B, Mackensen GB, Pineda J, et al. Anesthetic effects on cerebral metabolic rate predict histologic outcome from near-complete forebrain ischemia in the rat. *Anesthesiol J Am Soc Anesthesiol* 2000;93:431-436.
  55. Slupe AM, Kirsch JR. Effects of anesthesia on cerebral blood flow, metabolism, and neuroprotection. *J Cereb Blood Flow Metab* 2018;38:2192-2208.
  56. Gagnon L, Desjardins M, Jehanne-Lacasse J, et al. Investigation of diffuse correlation spectroscopy in multi-layered media including the human head. *Opt Express* 2008;16:15514.
  57. Baker WB, Parthasarathy AB, Ko TS, et al. Pressure modulation algorithm to separate cerebral hemodynamic signals from extracerebral artifacts. *Neurophotonics* 2015;2:035004.

58. Verdecchia K, Diop M, Lee A, et al. Assessment of a multi-layered diffuse correlation spectroscopy method for monitoring cerebral blood flow in adults. *Biomed Opt Express* 2016;7:3659.
59. Liemert A, Kienle A. Light diffusion in N-layered turbid media: steady-state domain. *J Biomed Opt* 2010;15:025003.
60. Liemert A, Kienle A. Light diffusion in a turbid cylinder II layered case. *Opt Express* 2010;18:9266-9279.
61. Hallacoglu B, Sassaroli A, Fantini S. Optical characterization of two-layered turbid media for non-invasive, absolute oximetry in cerebral and extracerebral tissue. *PLoS One* 2013: e64095.
62. Alexandrakis G, Busch DR, Faris GW, et al. Determination of the optical properties of two-layer turbid media by use of a frequency-domain hybrid Monte Carlo diffusion model. *Appl Opt* 2001;40:3810-3821.
63. Martelli F, Sassaroli A, Del Bianco S, et al. Solution of the time-dependent diffusion equation for layered diffusive media by the eigenfunction method. *Phys Rev E* 2003;67:056623.
64. Lian HE, Wesley B. Baker, Daniel Milej, et al. Noninvasive continuous optical monitoring of absolute cerebral blood flow in critically ill adults. *Neurophoton* 2018;5 (4):045006.